Available online at www.sciencedirect.com

ScienceDirect

Polymer 48 (2007) 5233–5240

polymer

www.elsevier.com/locate/polymer

Synthesis and thermal stability of hybrid fluorosilicone polymers

Michael P.C. Conrad [a], Molly S. Shoichet [a,b,c,*]

[a] Department of Chemical Engineering and Applied Chemistry, University of Toronto, 200 College Street, Toronto, ON, Canada M5S 3E5
[b] Institute of Biomaterials and Biomedical Engineering, University of Toronto, 164 College Street, Rm 407, Toronto, ON, Canada M5S 3G9
[c] Department of Chemistry, University of Toronto, 80 St. George Street, Toronto, ON, Canada M5S 3H6

Received 5 June 2007; accepted 7 July 2007

Abstract

Aromatic hybrid fluorosilicones, such as perfluorocyclobutane aromatic polyethers, have higher thermal stability than typical polysiloxanes. While these polyethers decompose by homolytic cleavage of the oxygen–perfluorocyclobutane bond, the enhanced thermal stability of the polyethers may, in part, arise from this oxygen through the anomeric effect. To determine the effect of the ether oxygen on thermal stability, two perfluorocyclobutane aromatic units, one with and one without the oxygen, were modeled. To confirm the results experimentally, a series of hybrid fluorosilicones based on the latter were synthesized by thermocyclodimerization of 1-bromo-4-(trifluorovinyl)benzene, metal–halogen exchange, and condensation with one of 1,3-dichlorotetramethyldisiloxane; 1,7-dichlorooctamethyltetrasiloxane; or chlorine-terminated poly(dimethylsiloxane). The degradation temperature ($T_{1\%}$) was lower (~240 °C) than the comparable polyethers (~430 °C). These results demonstrate the importance of the ether oxygen to the stability of perfluorocyclobutane aromatic polyethers through a number of effects including the anomeric effect and enhancing the strength of the silicon-aromatic bond.

Keywords: Fluorosilicone; Anomeric effect; Thermal stability

1. Introduction

Polysiloxanes are known for excellent low temperature capabilities as well as chemical and thermal stability. Despite this thermal stability, polysiloxanes are prone to depolymerization at elevated temperatures due to random chain scission [1]. To prevent chain scission, various polysilalkylene and polysilarylene siloxanes (hybrid silicones) have been synthesized. As described in a review by Guida-Pietrasanta and Boutevin [2], higher degradation temperatures can be achieved with alternating polymers. Additionally, aromatic polymers generally have greater thermal stability than their linear counterparts [3]. Thus, an exactly alternating polysilarylene siloxane should have the highest degradation temperature of the hybrid silicone class.

Fluoropolymers also have excellent thermal stability. Numerous authors [2,4–8] have synthesized hybrid fluorosilicones, wherein the fluorinated moiety is incorporated into the polymer backbone, to take advantage of this fact. Research by Boutevin and others [4–6] demonstrated that linear perfluorinated groups resulted in elevated degradation temperatures ($T_{10\%}$ ~ 285 °C). Moreover, hybrid fluorosilicones based on a perfluorocyclobutane aromatic ether showed even higher degradation temperatures ($T_{1\%}$ ~ 430 °C) [7,8], likely due to the incorporation of an aromatic versus a linear spacer between the siloxane repeats of the copolymer.

The thermal and oxidative decomposition of a thermoset based on the above perfluorocyclobutane aromatic polyether was studied (see Fig. 1) [9]. Kennedy et al. postulate that the mechanism for decomposition includes chain scission at either the benzylic carbon or oxygen and subsequent degradation of the resulting perfluorocyclobutene to hexafluorobutadiene. Thus, the oxygen appears to be one of the weak links

---

[*] Corresponding author. Donnelly Center for Cellular and Biomolecular Research, University of Toronto, 160 College St., Toronto, ON, Canada M5S 3E1. Tel.: +1 416 978 1460; fax: +1 416 978 8605.

E-mail address: molly@chem-eng.utoronto.ca (M.S. Shoichet).

0032-3861/$ - see front matter © 2007 Elsevier Ltd. All rights reserved.
doi:10.1016/j.polymer.2007.07.014

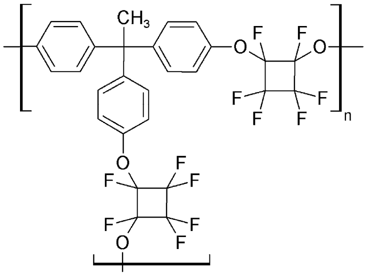

Fig. 1. Perfluorocyclobutane aromatic ether thermoset. Adapted from Kennedy et al. [9].

in the polymer structure. However, further examination of the perfluorocyclobutane aromatic ethers reveals that these polymers have the requisite structure, R–X–A–Y, to exhibit the anomeric effect [10]. In R–X–A–Y, R is a hydrogen or alkyl group (aromatic ring), X is an element with lone pairs (oxygen), A has an intermediate electronegativity (carbon), and Y is more electronegative than A (fluorine). The group or element in parentheses denotes the corresponding moiety in the perfluorocyclobutane aromatic ethers. In the case of these polyethers, the stereoelectronic interpretation of the anomeric effect is relevant. The lone pair on oxygen mixes with the antibonding C–F σ orbital, resulting in a lower energy molecular orbital. This, in turn, lowers the overall energy of the structure, giving greater stability to the polymer.

It was unclear whether removal of the ether oxygen would result in improved stability, due to prevention of homolytic cleavage, or reduced stability, due to elimination of the anomeric effect. We investigated this phenomenon, because materials based on perfluorocyclobutane aromatic polyethers show promise in numerous applications as: optical waveguides [11]; proton exchange membranes [12]; liquid crystals [13]; and coatings [14]. Two perfluorocyclobutane-based aromatic units, one with and one without oxygen (Fig. 2), were modeled and compared experimentally by synthesizing a series of hybrid fluorosilicones based on **M2**.

2. Experimental

2.1. Modeling

Compounds **M1** and **M2** were optimized for geometry in mechanics using augmented Allinger molecular mechanics force field (MM3) [16] parameters. Subsequently, the heat of formation for each of the molecules was calculated based on this optimized geometry in the CAChe semi-empirical molecular orbital package (MOPAC 2002 version 6.1.1.0) using parametric method 3 (PM3) [17] parameters.

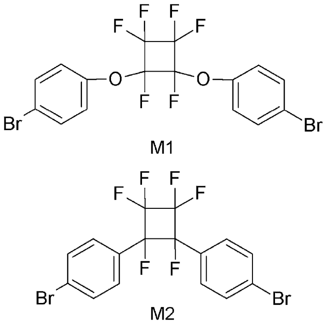

M1

M2

Fig. 2. Perfluorocyclobutane-based aromatic units. **M1** was synthesized by Ligon et al. [15]. **M2** was synthesized herein.

2.2. Materials

4-Bromoiodobenzene, *n*-butyl lithium, diethyl ether, anhydrous dimethylformamide tetrakistriphenylphosphine palladium(0), and zinc dust were purchased from Sigma-Aldrich (Ontario, Canada). Isopropanol, methanol, pentane, concentrated hydrochloric acid, and magnesium sulfate were purchased from Caledon (Ontario, Canada). Diethyl ether was dehydrated by passing over a neutral alumina column under an inert atmosphere. Inhibited bromotrifluoroethylene was purchased from SynQuest Laboratories Inc. (Alachua, Florida). The inhibitor was removed by inline filtration through chromatographic silica gel (200–425 mesh, Fisher Scientific, Ontario, Canada) prior to use. 1,3-Dichlorotetramethyldisiloxane, 1,7-dichlorooctamethyltetrasiloxane, and chlorine-terminated polydimethylsiloxane (425–600 g/mol) were purchased from Gelest Inc. (Tullytown, Pennsylvania). Zinc dust was activated using a literature procedure [18].

2.3. Characterization

^{1}H NMR at 400 MHz, ^{19}F NMR at 376 MHz and ^{29}Si NMR at 79 MHz spectra were obtained with a Varian Mercury 400 MHz system with chloroform-*d* as the solvent. Infrared spectra were obtained for neat liquids placed on a Harrick Split Pea™ system equipped with a Si window attached to a Nicolet Avatar 370 MCT FT-IR spectrophotometer. The gas chromatography/mass spectrometry (GC/MS) data were obtained from an HP5890 II gas chromatograph coupled with a VG Trio 1000 mass spectrometer. The method used was electron ionization at an energy level of 70 eV. For the polymer samples, only the mass spectra were obtained. An aliquot of polymer was placed into a small glass capillary tube, heated from 100 to 450 °C at 0.5 °C/s and the degradation products analyzed. Polymer molar mass was measured by gel permeation chromatography (GPC, Viscotek VE2001 GPCmax) equipped with a triple detector array (Viscotek TDA302) for refractive index, light scattering (right and low angle) and viscosity. Using THF as the mobile phase at a flow rate of 1 mL/min, polymer molar mass was calculated relative to polystyrene standards using two ViscoGEL™ columns (I-MBHMW-3807 and I-MBLMW-3807) in series.

Glass transition temperature (T_g) was measured using a TA Q1000 differential scanning calorimeter (DSC), under nitrogen atmosphere, at a heating rate of 10 °C/min and scanning range of −90 to 125 °C. Thermogravimetric analysis (TGA) was performed using a TA Q50 instrument under a compressed air atmosphere at a heating rate of 5 °C/min and scanning range of 25–600 °C.

2.4. Synthesis of monomers

1-Bromo-4-(trifluorovinyl)benzene (**I2**) was synthesized as shown in Scheme 1, based on work by Burton and coworkers [19–22] and specifically the method outlined by Heinze and Burton [19] involving bromotrifluoroethylene was used. In an inert atmosphere, activated zinc powder (9.3 g, 142 mmol) and a magnetic stir bar were placed in a 250 mL, three-neck round-bottom flask. This was connected to a dry ice/isopropanol condenser. Anhydrous dimethylformamide (DMF) (99.4 g) was added by cannula. A gas cylinder containing bromotrifluoroethylene was connected to both the flask and a vacuum line through a series of Swagelok fittings. The gas line was evacuated and purged with nitrogen. Bromotrifluoroethylene (**2**) (34.4 g, 201 mmol) was slowly added while maintaining the temperature of the flask between 0 and 10 °C with an ice bath; a brown mixture resulted. The amount of gas added was determined by weight difference. After the full amount of gas was added, the mixture was brought to room temperature and stirred for an additional 4 h.

In an inert atmosphere, a second 250 mL, three-neck, round-bottom flask with a magnetic stir bar was charged with 4-bromoiodobenzene (24.8 g, 109 mmol) and tetrakistriphenylphosphine palladium ($Pd(PPh_3)_4$, 2.0 g, 2 mol% based on the aryl iodide). The zinc reagent formed in the previous step was transferred to this flask under inert atmosphere by cannula. The reaction was stirred overnight under an inert atmosphere at 30 °C.

The mixture was extracted with 25 mL of pentane five times (total of 125 mL). The resulting yellow solution was washed with 25 mL of 5% HCl three times and subsequently dried over magnesium sulfate. The solution was filtered through a silica gel column and concentrated. The residue was distilled under high-vacuum (25 mm Hg and 45 °C) to yield **I2** (16.4 g, 79% – based on the aryl iodide). The synthesis was confirmed by ^1H and ^{19}F NMR, FT-IR spectroscopy and GC/MS. ^1H NMR (400 MHz, $CDCl_3$) δ: 7.54 (d, 2H, Ar), 7.32 (d, 2H, Ar). ^{19}F NMR (375 MHz, $CDCl_3$) δ: −99.0 (dd, F_{cis}), −113.8 (dd, F_{trans}), −177.5 (dd, F_α); $J_{cis-trans} = 69$ Hz, $J_{trans-\alpha} = 110$ Hz, $J_{cis-\alpha} = 33$ Hz. IR (neat) 1759 (vs, $CF_2{=}CF-$), 1593 (m), 1491 (m), 1402 (m), 1290 (vs, C–F), 1151 (s), 1072 (m), 983 (s), and 825 (s) cm^{-1}. Mass spectrum: $C_8F_3H_4^{81}Br^+$, 238 (100); $C_8F_3H_4^{79}Br^+$, 236 (100); $C_8F_3H_4^+$, 157 (71); $C_8F_2H_3^+$, 137 (65); $C_7FH_4^+$, 107 (62).

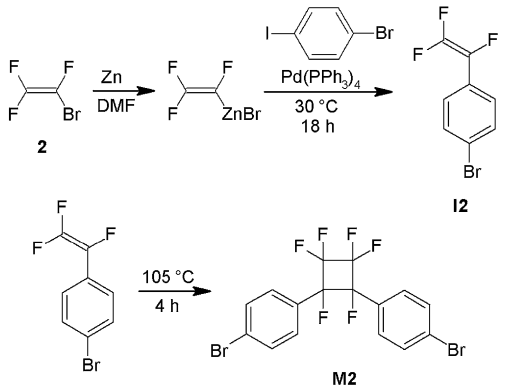

Scheme 1. Synthesis of monomers.

1,1′-(1,2,3,3,4,4-Hexafluorocyclobutane-1,2-diyl)bis(4-bromobenzene) (**M2**) was synthesized according to Scheme 1. A three-neck, 100 mL round-bottom flask was charged with 2.8 g (6.0 mmol) of **I2**, sealed, purged with nitrogen, and heated to 105 °C for 4 h. Any remaining **I2** was removed through vacuum evaporation (50 °C, 30 mm Hg). This resulted in a *trans*:*cis* ratio of 56:44 (according to Ligon et al. [15]), as determined by comparing the integration of the aromatic peaks in ^1H NMR, and a yield of 86%. The synthesis of **M2** was confirmed by ^1H and ^{19}F NMR, FT-IR spectroscopy and GC/MS. ^1H NMR (400 MHz, $CDCl_3$) δ: 7.62 (d, 2H, Ar), 7.46 (d, 2H, Ar), 7.41 (d, 2H, Ar), 7.10 (d, 2H, Ar). ^{19}F NMR (375 MHz, $CDCl_3$) δ: −125.1 (m, $4F_a$), −164.1 (d, $2F_b$). IR (neat) 1593 (m), 1494 (s), 1369 (s), 1254 (m), 1185 (vs), 1076 (m), 1011 (m), 879 (m), 857 (s), 820 (m), and 794 (m) cm^{-1}. Mass spectrum: $C_8F_3H_4^{81}Br^+$, 238 (100); $C_8F_3H_4^{79}Br^+$, 236 (98); $C_8F_3H_4^+$, 157 (45); $C_8F_2H_3^+$, 137 (30); $C_7FH_4^+$, 107 (48).

2.5. Synthesis of polymers

The hybrid fluorosilicones are synthesized by reacting *n*-BuLi with **M2** and subsequently forming a condensation polymer by adding a dichlorosiloxane as shown in Scheme 2. A typical experiment is as follows. In a three-neck 100 mL round-bottom flask fitted with two equalizing addition funnels 1.94 g (4.1 mmol) of **M2** was dissolved in 3.6 g of anhydrous diethyl ether. This mixture was cooled to −78 °C using an acetone/liquid nitrogen bath. The addition funnels were charged with 2.27 g (8.7 mmol) of *n*-BuLi (2.5 M in hexanes) and 0.85 g (4.2 mmol) of 1,3-dichlorotetramethyldisiloxane (**a**), respectively. The *n*-BuLi was added dropwise to **M2** while maintaining the temperature at −78 °C. The reaction mixture turned orange and was held at −78 °C for approximately 1 h. The siloxane was then added dropwise. Afterwards, the mixture was brought to room temperature and stirred for at least

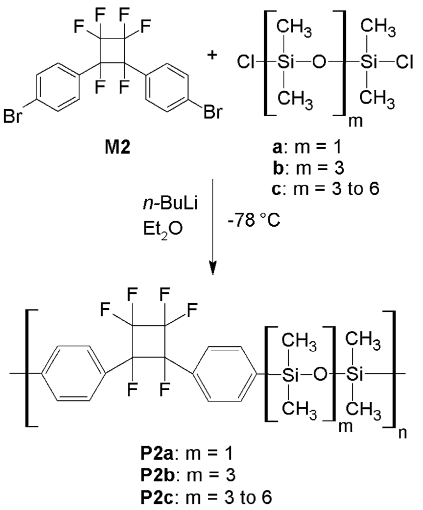

Scheme 2. Synthesis of polymers.

1 h. Any precipitate was removed by filtration and solvent was removed through rotary evaporation. The crude product was dissolved in ether and precipitated in methanol. The polymer was redissolved in ether, dried over $MgSO_4$, filtered and any remaining ether was removed by vacuum drying. This resulted in 166 mg (0.3 mmol, 9%) of a tacky, orange solid (**P2a**). The synthesis of **P2a** was confirmed through ^1H, ^{19}F, and ^{29}Si NMR. ^1H NMR (400 MHz, $CDCl_3$) δ: 7.47 (m, 8H, Ar), 0.21 (m, 12H, $OSi(Me_2)Ar$). ^{19}F NMR (375 MHz, $CDCl_3$) δ: −125.6 (m, 4F), −163.5 (d, 2F). ^{29}Si NMR (79 MHz, $CDCl_3$) δ: −0.64 (s, 2Si, $OSi(Me_2)Ar$).

The above reaction was also completed using 3.5 g (7.4 mmol) of **M2**, 4.9 g (17.7 mmol) of *n*-BuLi (2.5 M in hexanes) and 2.7 g (7.7 mmol) of 1,7-dichlorotetramethyldisiloxane (**b**), yielding 990 mg (1.7 mmol, 23%) of a tacky, orange solid (**P2b**). The synthesis of **P2b** was confirmed through ^1H, ^{19}F, and ^{29}Si NMR. ^1H NMR (400 MHz, $CDCl_3$) δ: 7.63 (d, 2H, Ar), 7.55 (d, 2H, Ar), 7.44 (d, 2H, Ar), 7.20 (d, 2H, Ar), 0.28 (m, 12H, $OSi(Me_2)Ar$), 0.02 (m, 12H, $OSi(Me_2)O$). ^{19}F NMR (375 MHz, $CDCl_3$) δ: −124.9 (m, 4F), −163.3 (d, 2F). ^{29}Si NMR (79 MHz, $CDCl_3$) δ: −2.53 (s, 2Si, $OSi(Me_2)Ar$), −20.22 (s, 2Si, $OSi(Me_2)O$).

The synthesis of **P2c** is similar to that of **P2a** using 4.75 g (10 mmol) of **M2**, 5.37 g (21 mmol) of *n*-BuLi (2.5 M in hexanes), and 5.13 g (10 mmol) of chlorine-terminated polydimethylsiloxane (**c**) yielding 2.42 g (3.2 mmol, 32%) of a tacky, orange solid (**P2c**). The synthesis of this polymer was also confirmed through ^1H, ^{19}F, and ^{29}Si NMR. The NMR results for **P2c** are indistinguishable from those for **P2b**.

3. Results and discussion

3.1. Modeling

The heats of formation for **M1** and **M2** are −1140 kJ/mol and −815 kJ/mol, respectively. These were calculated based on the optimized geometry in MOPAC using PM3 parameters. Therefore, 1,1′-[(1,2,3,3,4,4-hexafluorocyclobutane-1,2-diyl)bis(oxy)]bis(4-bromobenzene) (**M1**) is more stable by 325 kJ/mol. The majority of this stability arises from the inclusion of oxygen in **M1**. As shown in Table 1, the average decrease in ΔH_f is 150 kJ/mol per oxygen, which results in a difference of 300 kJ/mol between **M1** and **M2**.

Table 1
Effect of oxygen on ΔH_f taken from Refs. [23,24]

Compounds	ΔH_f (kJ/mol)	$\Delta\Delta H_f$ (kJ/mol)	ΔH_f per oxygen added (kJ/mol)
Methane/methanol	−75/−201	126	126
Ethane/ethanol	−85/−235	150	150
Ethane/ethylene glycol	−85/−390	305	153
Propane/propanol	−104/−269	165	165
Propane/glycerol	−104/−586	482	161
Butane/diethyl ether	−126/−253	109	109
Benzene/phenol	83/−96	179	179

Compound **M1** also displays the requisite structure for the anomeric effect and should be stabilized by an additional 5–10 kJ/mol. Interestingly, Ligon et al. [15] show the dihedral angle of the cyclobutane ring for *trans*-**M1** to be 16° and for *cis*-**M1** to be 4°. The dihedral angle for perfluorocyclobutane is $20 \pm 4°$ [25]. Thus, while the dihedral angle for the *trans*-**M1** falls within this range, *cis*-**M1** has additional ring strain from adopting the planar form. Modeling of **M2** suggests that both the *cis* and *trans* forms adopt the puckered conformation and should be present in nearly equal amounts, yet the ratio of *trans*:*cis* is 56:44 compared with 53:47 for **M1**. The relative increase in the *cis* isomer for **M1** may be due to stabilization of the planar form by the anomeric effect as the barrier between the planar and puckered conformation is 6 kJ/mol [25].

3.2. Polymerization

A family of hybrid fluorosilicones was synthesized by a condensation polymerization between **M2** and dichlorosiloxanes of varying lengths. Results are summarized in Table 2.

The synthetic scheme used in this work is similar to that demonstrated by Smith and Babb [7] and Rizzo and Harris [8]. Smith and Babb performed the condensation of the dichlorosiloxane with the 1-bromo-4-(trifluorovinyloxy)benzene prior to thermocyclopolymerization. While this gives a large degree of control over the final molecular weight of the product, it leads to a somewhat reduced molecular weight of 12,000–20,000 g/mol depending on the siloxane linker. However, this method is unsuitable for polymers based on trifluorovinylbenzene. The condensation cannot occur prior to thermocyclopolymerization because the reaction between the styrene and lithium-based nucleophiles leads to the formation of a stilbene [26]. Rizzo and Harris reverse the order of the condensation and thermocyclopolymerization achieving higher molecular weights of 52,000–58,000 g/mol by using silanol self-condensation as the polymerization mechanism. Yet they also attach the silicon to the aromatic ring prior to thermocyclodimerization, which will lead to the formation of a stilbene for fluorinated styrene monomers. Stilbene formation can be completely avoided by the thermocyclodimerization of the styrene [27] prior to the addition of the nucleophile, removing the reactive fluorinated alkene.

Rizzo and Harris also demonstrate that the effect of changing the condensation mechanism can be substantial. Moving from thermocyclodimerization to silanol self-condensation

Table 2
Summary of molecular weight and thermal properties for hybrid fluorosilicones, **P2a**–**P2c**

Polymer	M_w[a] (g/mol)	M_n[a] (g/mol)	M_w/M_n	T_g[b] (°C)	$T_{1\%}$[c] (°C)
P2a	1900	1500	1.3	−7	237
P2b	9300	2800	3.3	−55	236
P2c	18,000	7300	2.5	−77	241

[a] Determined by GPC using polystyrene standards in THF at 35 °C.

[b] Mid-point in change in slope in DSC thermogram obtained with a heating rate of 10 °C/min.

[c] Temperature at which 1% weight loss was seen during TGA under air at a heating rate of 5 °C/min.

increases the molecular weight by a factor of 3. However, they use chlorodimethylsilane to form their Si to aromatic attachment. While the Si–H is a less reactive leaving group than Si–Cl [28], the possibility exists for premature polymerization. Particularly since the hydrogen most readily reacts when attached to an arylsilane [28]. This was avoided herein by using dichlorosiloxanes and thus forming the desired polymer in one step. A drawback to changing the condensation mechanism is a severe reduction in molecular weight which can be seen by comparing **P2b** ($M_n = 2800$ g/mol) to the equivalent perfluorocyclobutane aromatic polyether ($M_n = 58{,}000$ g/mol) [8].

This reduction in molecular weight is due to the change in condensation mechanism from the self-condensation of a disilanol to a metal–halogen exchange reaction. In the former, as well as the work by Smith and Babb [7], an A–B monomer is used and the molecular weight of the polymer is dependent only upon the extent of reaction, *p*. However, in the latter (our case), the chain-forming reaction occurs between two monomers: A–A and B–B. The molecular weight depends on both the extent of reaction and the ratio of the monomers, *r*, as seen in Eq. (1). Since Rizzo and Harris [8] form high molecular weight polymer through the condensation of a dichlorosiloxane and disilanol, our inability to form high molar mass polymer results likely from either low efficiency of the metal–halogen exchange reaction or competing side reactions that reduce the molecular weight of the polymers synthesized herein.

$$\overline{DP}_n = \frac{1+r}{1+r-2rp} \qquad (1)$$

There are two metal–halogen exchange reactions that occur in Scheme 2: the exchange between *n*-BuLi and **M2** and the exchange between lithiated **M2** (Li-**M2**) and a dichlorosiloxane. Poor efficiency, ε_1, of the first reaction will result in a reduction of *r* as it is not the ratio of **M2** to the dichlorosiloxane but rather the ratio of Li-**M2** to dichlorosilxoane that determines *r*. The minimum *r* value, $r_{\min}$, can be calculated by setting $p = 1$ in Eq. (1), i.e. the reaction between Li-**M2** and the dichlorosiloxane is quantitative. This results in $r_{\min}$ values of 0.74, 0.80 and 0.90 for **P2a**, **P2b**, and **P2c**, respectively, which are lower than the *r* values calculated from the monomer masses (0.98, 0.96, and 0.996). The difference is the efficiency of the lithium–metal exchange, since $r_{\min} = r\varepsilon_1$, and the calculated ε_1 is between 76 and 92%. This corresponds well with similar reactions between *t*-BuLi and brominated trifluorovinyloxybenzene where yields of 58–78% are seen [29].

The *r* value may also be reduced if the metal–halogen exchange only occurs at one of the bromines on **M2**. However, work by Larsen and Jorgensen [30] on calixarenes show that the number of bromines substituted corresponds to the number of equivalents of *n*-BuLi used, and thus, a molar ratio of **M2**:*n*-BuLi of 1:2 should result in a dilithium product. In contrast, Beak and Liu [31] show a mix of dibromo, monobromo and bromine-free products for a metal–halogen exchange, yet this occurs with *t*-BuLi. They add only one equivalent of *t*-BuLi whereas due to the equilibrium nature of the metal–halogen exchange reaction a second equivalent of *t*-BuLi is required to make the reaction irreversible [32].

Reversibility of the lithium–halogen exchange reaction suggests that the reaction between *n*-BuLi and **M2** should proceed at a higher efficiency than that between Li-**M2** and the dichlorosiloxane since the K_{eq}s are ~7500 and 1 [32], respectively. Poor efficiency of the second metal–halogen exchange between Li-**M2** and the dichlorosiloxane will affect the extent of reaction, *p*, and thus, the minimum calculated extent of reaction, $p_{\min}$, should be less than ε_1. Interestingly, $p_{\min}$, calculated by setting $r = 1$, is 0.85, 0.89, and 0.95 for **P2a**, **P2b**, and **P2c**. While these extent of reactions would be satisfactory for a wide variety of chemical reactions, for condensation polymerizations *p* is typically greater than 98–99% to achieve high molecular weight polymers [33].

The alternative to poor lithium–halogen exchange efficiency is the presence of side reactions which can reduce both *r* and *p*. This possibility was examined by running the polymerization without one of the monomers, i.e. one reaction with only **M2** and one reaction with only the dichlorosiloxane. There appears to be no side reaction in the lithium–halogen exchange between *n*-BuLi and **M2** although there is evidence of leftover **M2**. This is not unexpected as it is unlikely that the reaction is quantitative as seen by both calculations of the lithium efficiency and the results of Ji et al. [29].

The second reaction results in the formation of a butyl-substituted siloxane, likely α,ω-butylsiloxane. This will reduce the expected amount of dichlorosiloxane available for reaction; however, this does not necessarily reduce *r* for the overall reaction. As less **M2** undergoes the lithium–halogen exchange, i.e. a lower ε_1, *r* for the reaction will be reduced. Yet a similar reduction in the amount of dichlorosiloxane by side reactions will increase *r* since it is determined by the ratio of the reactive groups rather than their absolute number. A more detrimental effect of this side reaction is substitution of the chlorine by the butyl group which represents an end-capping reaction. This will reduce the molecular weight of the polymers and may also affect the polydispersity.

The classical PDI for condensation polymerizations is 2.0. However, none of the polymers synthesized herein have PDIs which approach this number. Low polydispersities have previously been seen by Rizzo and Harris [8] and were attributed to fractionation during the methanol precipitation. This is likely the case for **P2a**. The high polydispersity for **P2b** is attributed to a low molecular weight tail, which may arise from two sources: cyclic oligomers and a capping reaction. No evidence of cyclics was found in the GPC data, which suggests that the latter is contributing to the broader molecular weight distribution. Polymer **P2c** most closely approaches the theoretical PDI value. In this case, the difference from theoretical is accredited to the dichlorosiloxane having a molecular weight range rather than a specific molecular weight.

While the polymerization scheme presented herein prevents the formation of a stilbene and potential premature polymerization, using lithium–halogen exchange as the condensation mechanism appears unsuitable for this particular combination of monomers. The efficiency of the reaction as well as potential side reactions results in a significantly lowered molecular weight. However, this does not preclude an examination of the thermal properties of the oligomers formed.

3.3. Thermal properties

The T_g of a polymer is affected by polymer chain flexibility, with increased flexibility resulting in a lower T_g. Similarly for copolymers, increasing the weight percent of the more flexible component yields a decrease in T_g. This effect has been observed in polysilarylene siloxanes [34] and perfluorocyclobutane aromatic polyethers [8,35]. The glass transition temperatures of the hybrid fluorosilicones synthesized herein follow the expected pattern of decreasing T_g with increasing weight percentage of siloxane, from **P2a** (−7 °C/30 wt%) to **P2b** (−55 °C/47 wt%) to **P2c** (−77 °C/58 wt%), as shown in Fig. 3. These results are tempered by the low molecular weight of the three polymers. Rizzo and Harris [8] show that for a polymer similar to **P2a**, a molecular weight of 50,000 g/mol is required before T_g is independent of molecular weight. This molecular weight independent T_g (T_g^∞) can be calculated based on Eq. (2) [33]:

$$T_g = T_g^\infty - \frac{K}{M} \tag{2}$$

where T_g is the glass transition temperature of the polymer at molecular weight M, and K is a constant. The K for the polymers synthesized herein is unknown, but can be determined using work by Boyer [36]. Since the T_g of the polymers is known for a given M, there is only one point on the curve presented by Boyer, which relates T_g^∞ and K, that will satisfy Eq. (2). This results in K values of 80,000, 20,000, and 10,000 g K/mol for **P2a**, **P2b**, and **P2c**, respectively. Using the same methodology gives $K = 60{,}000$ g K/mol for the polymer synthesized by Rizzo and Harris, which corresponds with their reported experimental value of 50,000 g/mol. The corrected glass transition temperatures still follow the expected pattern of decreasing T_g with increasing weight percent siloxane, from **P2a** (46 °C) to **P2b** (−48 °C) to **P2c** (−76 °C); however, the T_g values are higher than those measured experimentally.

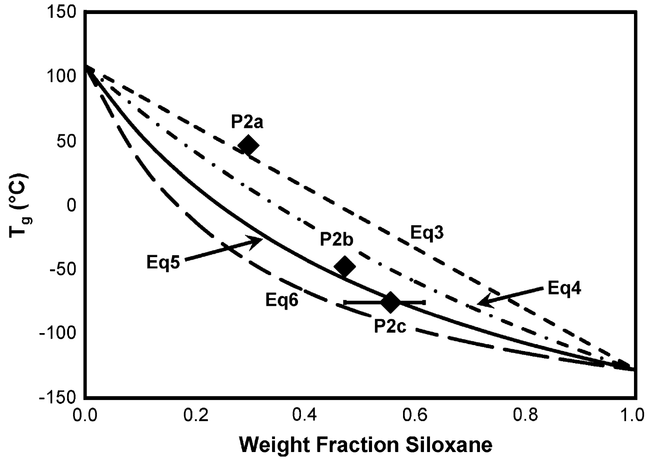

Fig. 3. Comparison of corrected experimental (◆) to calculated glass transition temperatures according to each of Eqs. (3)–(6). The T_g values were calculated using a T_{g1} of −128 °C for polydimethlysiloxane and the experimental T_gs from DSC at a heating rate of 10 °C/min in N_2, 2nd run.

The effect of copolymer composition on T_g can be determined through a number of equations: a simple rule of mixtures, Eq. (3); a logarithmic rule of mixtures, Eq. (4); the Fox equation, Eq. (5); and the more general case from which the logarithmic rule of mixtures and the Fox equation are derived, Eq. (6), all of which are shown below [33]:

$$T_g = w_1 T_{g1} + w_2 T_{g2}, \tag{3}$$

$$\ln T_g = w_1 \ln T_{g1} + w_2 \ln T_{g2}, \tag{4}$$

$$\frac{1}{T_g} = \frac{w_1}{T_{g1}} = \frac{w_2}{T_{g2}}, \tag{5}$$

$$\ln\left(\frac{T_g}{T_{g1}}\right) = \frac{w_2 \ln\left(T_{g2}/T_{g1}\right)}{w_1\left(T_{g2}/T_{g1}\right) + w_2} \tag{6}$$

where T_g is the T_g of the copolymer; w_1 and w_2 are the weight percents of the respective components; and T_{g1} and T_{g2} are the T_gs of the respective components.

These equations can be used to obtain a value for T_{g2}, since the perfluorocyclobutane aromatic homopolymer is unavailable. Each of the equations should result in the same T_{g2} since they are modeling the same copolymer system. Thus, by minimizing the total error associated with all of the curves, in effect minimizing the area bounded by the Eqs. (3)–(6), a T_{g2} of 108 °C is obtained as shown in Fig. 3 (NB: calculations were done in Kelvin but plotted in °C for ease of comparison with the literature). Fig. 3 also shows that the T_g for **P2a** does not fall within the boundary of the equations. This is likely due to the extremely low molecular weight of **P2a** which leads to an overestimate of T_g^∞. A similar calculation, i.e. minimizing the area bounded by Eqs. (3)–(6) as above, for the equivalent polyethers gives a T_{g2} of 116 °C. For comparison, the T_g of the polyether homopolymer is 170 °C, which shows that this methodology underestimates the true T_g of the perfluorocyclobutane component. However, without the homopolymer available this represents the best estimate for T_{g2}. By either comparison, the T_g of the polyethers is greater than that of the polymers without the ether oxygen. Therefore, the incorporation of the ether oxygen, rather than enhancing the flexibility of the polymer backbone as is typically the case, appears to stiffen the perfluorocyclobutane aromatic polyethers. The increase in T_g for the polyether is also seen when comparing the T_g of **P2b** at −48 °C (47 wt% siloxane) with an equivalent polyether at −12 °C and 45 wt% siloxane [8].

This may be explained by the anomeric effect, which provides enhanced stability to certain molecular conformations over others, for example, the preference for the axial rather than the equatorial position for alkoxy substituted pyranose rings [10]. As mentioned, the perfluorocyclobutane aromatic polyethers have the requisite structure to exhibit the anomeric effect. Thus, some conformations of these polymers will be preferred over others. The stabilization of these conformations represents an additional barrier to molecular movement, which increases the T_g of the polyethers above that of polymers without the ether oxygen.

The greater thermal stability of the perfluorocyclobutane aromatic polyethers [35] was confirmed experimentally. The polymers based on **M1** degraded at much higher temperatures ($T_{1\%} \sim 432$ °C in N_2) than those in this work ($T_{1\%} \sim 240$ °C in air). This comparison is valid, despite the change in atmosphere, as research has shown little to no difference in the onset degradation temperature when the atmosphere is changed from air to N_2 [9]. Additionally, **P2b** was run in N_2 and gave $T_{1\%}$ of 212 °C. Air was considered the more industrially relevant of the two and all subsequent TGAs were run in this atmosphere.

While the length of siloxane linkage affected T_g, it had little to no effect on the $T_{1\%}$ as shown in Fig. 4. The lack of effect on $T_{1\%}$ for varying siloxane weight percent was also seen for perfluorocyclobutane aromatic polyethers [35]. Additionally, $T_{1\%}$ is independent of molecular weight for the polymers in this work as shown in Table 2. This is contrary to the results for a series of linear polysiloxanes where a reduction in molecular weight led to a reduction in $T_{1\%}$, which suggests that the lower decomposition temperature measured for the hybrid fluorosilicones herein is due to the polymeric structure rather than the lower molecular weight. It should be noted that trace amounts of $MgSO_4$ may catalyze the decomposition [28], but this was removed during purification and would unlikely result in nearly identical degradation temperatures.

To determine the initial decomposition mechanism, polymers **P2b** and **P2c** were heated at 0.5 °C/min from 100 to 450 °C, and the products were analyzed by mass spectrometry. In the case of **P2c**, the first degradation product observed at 322 °C is $[Si(Me)_2O]_4Si(Me)_2$ in addition to lower order siloxanes with 3 and 2 $[Si(Me)_2O]$ units. This suggests that the initial decomposition step is cleavage of the Si–Ar bond. This is confirmed by the degradation of **P2b** where $[Si(Me)_2O]_3$-$Si(Me)_2$ is the only product observed until 299 °C. The lack of higher molecular weight siloxanes, as seen in **P2c**, suggests that this degradation is also the result of Si–Ar bond cleavage since the siloxane linker in **P2b** consisted of a linear tetrasiloxane. The Si–Ar bond cleaved is likely that associated with the end groups. The lack of higher molecular weight siloxanes also suggests that linear siloxanes are not formed during polymerization.

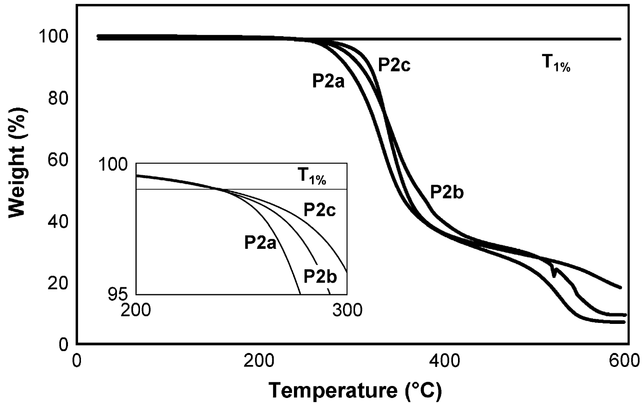

Fig. 4. Thermal gravimetric analysis of hybrid fluorosilicones, **P2a**–**P2c**; 5 °C/min in air.

At higher temperatures, the presence of a butyl siloxane provides experimental evidence for the postulated capping mechanism, where unreacted *n*-BuLi reacts with the growing chain, reducing the polymer molecular weight. Above 330 °C, the first indication of a trifluorostyrene resulting from the cleavage of the perfluorocyclobutane ring is found. This includes traces of the brominated starting product, **M2**, confirming the likelihood of less than 100% efficiency for the lithium–halogen exchange reaction. At temperatures greater than 440 °C, the bond between the aromatic and perfluorocyclobutane rings is broken. Therefore, the postulated mechanism for decomposition is cleavage of the Si–Ar bond, followed by splitting of the perfluorocyclobutane ring, and breaking of the aromatic/perfluorocyclobutane C–C bond.

If the Si–Ar cleavage is the initial decomposition step, one would expect the degradation temperature of the polymers synthesized herein to be comparable to the aromatic polyethers. This is not the case, which implies that the Si–Ar bond in the polyethers must be stronger. Work by Hehre et al. [37] supports this hypothesis. They show that the π-electron density on the aromatic carbon *para* to an oxygen substituent is greater than the electron density of the one opposite to an alkyl fluoride (see Fig. 5). This increased electron density on the carbon strengthens the Si–Ar bond, and the incorporation of oxygen has led to a second possible stabilization effect for these polymers.

4. Conclusion

The effect of the ether oxygen on the stability of perfluorocyclobutane aromatic polyethers has been determined. Molecular modeling shows that an oxygen link between the perfluorocyclobutane and phenyl rings results in a more stable structure versus one with a direct perfluorocyclobutane to phenyl bond, with heats of formation of −1140 kJ/mol and −815 kJ/mol, respectively. This was confirmed experimentally by synthesizing a series of new fluorosilicones by the thermocyclodimerization of 1-bromo-4-(trifluorovinyl)benzene followed by condensation with a number of dichlorosiloxanes and comparing the thermal stability of these polymers to

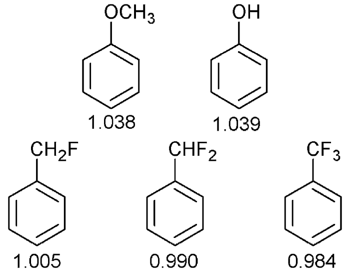

Fig. 5. π-Electron density of carbon *para* to functional group on substituted benzenes. Adapted from Hehre et al. [37].

perfluorocyclobutane aromatic polyethers [8,35]. In both modeling and experimental results, the polymers without the ether oxygen have lower thermal stability. This decrease in thermal stability does not arise from either an increased weight percent of the siloxane component or a decrease in molecular weight. The reduced thermal stability is due to the removal of the ether oxygen. While the removal of this oxygen eliminates a possible decomposition pathway, it also eliminates the anomeric effect and the greater stability of the silicon-aromatic bond.

Acknowledgements

The authors would like to acknowledge Dr. Bilal Baradie and Dr. Jordan Wosnick for their assistance and expertise. The authors would also like to acknowledge Xerox Research Centre of Canada, the Natural Sciences and Engineering Research Council of Canada, the Ontario Graduate Scholarship, and the Colin Hahnemann Bayley Fellowship for funding.

References

[1] Dvornic PR, Lenz RW. High temperature siloxane elastomers. New York: Huthig & Wepf Verlag Basel; 1990.
[2] Guida-Pietrasanta F, Boutevin B. Advanced Polymer Science 2005;179: 1–27.
[3] Conley RT. Molecular structure and stability criteria. In: Conley RT, editor. Thermal stability of polymers. New York: Marcel Dekker, Inc.; 1970. p. 21–45.
[4] Boutevin B, GuidaPietrasanta F, Ratsimihety A, Caporiccio G. Main Group Metal Chemistry 1997;20(2):133–6.
[5] Ameduri B, Boutevin B, GuidaPietrasanta F, Manseri A, Ratsimihety A, Caporiccio G. Journal of Polymer Science Part A: Polymer Chemistry 1996;34(15):3077–90.
[6] Boutevin B, Caporiccio G, Guida-Pietrasanta F, Ratsimihety A. Macromolecular Chemistry and Physics 1998;199(1):61–70.
[7] Smith DW, Babb DA. Macromolecules 1996;29(3):852–60.
[8] Rizzo J, Harris FW. Polymer 2000;41(13):5125–36.
[9] Kennedy AP, Babb DA, Bremmer JN, Pasztor AJ. Journal of Polymer Science Part A: Polymer Chemistry 1995;33(11):1859–65.
[10] Juaristi E, Cuevas G. The anomeric effect. Ann Arbor: CRC Press; 1995.
[11] Wong S, Ma H, Jen AKY, Barto R, Frank CW. Macromolecules 2003;36(21):8001–7.
[12] Perpall MW, Smith DW, DesMarteau DD, Creager SE. Polymer Reviews 2006;46(3):297–313.
[13] Jin JY, Smith DW, Glasser S, Perahia D, Foulger SH, Ballato J, et al. Macromolecules 2006;39(14):4646–9.
[14] Smith DW, Babb DA, Shah HV, Hoeglund A, Traiphol R, Perahia D, et al. Journal of Fluorine Chemistry 2000;104(1):109–17.
[15] Ligon SC, Krawiec M, Kitaygorodskiy A, Smith DW. Journal of Fluorine Chemistry 2003;123(1):139–46.
[16] Allinger NL, Yuh YH, Lii JH. Journal of the American Chemical Society 1989;111(23):8551–66.
[17] Stewart JJP. Journal of Computational Chemistry 1989;10(2):209–20.
[18] Tran-Van F, Garreau S, Louarn G, Froyer G, Chevrot C. Journal of Materials Chemistry 2001;11(5):1378–82.
[19] Heinze PL, Burton DJ. Journal of Fluorine Chemistry 1986;31(1): 115–9.
[20] Heinze PL, Burton DJ. Journal of Organic Chemistry 1988;53(12): 2714–20.
[21] Anilkumar R, Burton DJ. Tetrahedron Letters 2002;43(15):2731–3.
[22] Raghavanpillai A, Burton DJ. Journal of Organic Chemistry 2004; 69(21):7083–91.
[23] Winnick J. Chemical engineering thermodynamics: an introduction to thermodynamics for undergraduate engineering students. New York: Wiley; 1997.
[24] Smith JM, Van Ness HC, Abbott MM. Introduction to chemical engineering thermodynamics. 5th ed. Toronto: The McGraw-Hill Companies, Inc.; 1996.
[25] Cotton FA, Frenz BA. Tetrahedron 1974;30(12):1587–94.
[26] Souzy R, Ameduri B, Boutevin B. Progress in Polymer Science 2004;29(2):75–106.
[27] Tellier F, Sauvetre R, Normant JF, Dromzee Y, Jeannin Y. Journal of Organometallic Chemistry 1987;331(3):281–98.
[28] Brook MA. Silicon in organic, organometallic, and polymer chemistry. Toronto: John Wiley & Sons, Inc.; 2000.
[29] Ji J, Narayan-Sarathy S, Neilson RH, Oxley JD, Babb DA, Rondan NG, et al. Organometallics 1998;17(5):783–5.
[30] Larsen M, Jorgensen M. Journal of Organic Chemistry 1996;61(19): 6651–5.
[31] Beak P, Liu C. Tetrahedron 1994;50(20):5999–6004.
[32] Clayden J. Organolithiums: selectivity for synthesis. New York: Pergamon; 2002.
[33] Odian G. Principles of polymerization. 4th ed. Hoboken, NJ: John Wiley & Sons, Inc.; 2004.
[34] Dvornic PR, Lenz RW. Macromolecules 1992;25(14):3769–78.
[35] Smith DW, Ji J, Narayan-Sarathy S, Neilson RH, Babb DA. In: Clarson SJ, editor. Fluorosilicones containing the perfluorocyclobutane aromatic ether linkage. Silicones and silicone-modifided materials, vol. 729. Washington, DC: American Chemical Society; 2000. p. 308–21.
[36] Boyer RF. Macromolecules 1974;7(1):142–3.
[37] Hehre WJ, Radom L, Pople JA. Journal of the American Chemical Society 1972;94(5):1496–504.